Aerosol Science and Technology

ISSN: (Print) (Online) Journal homepage: www.tandfonline.com/journals/uast20

Understanding the influence of atomizing power on electronic cigarette aerosol size and inhalation dose estimation

Jinho Lee, Wei-Chung Su & Inkyu Han

To cite this article: Jinho Lee, Wei-Chung Su & Inkyu Han (2023) Understanding the influence of atomizing power on electronic cigarette aerosol size and inhalation dose estimation, Aerosol Science and Technology, 57:7, 633-644, DOI: 10.1080/02786826.2023.2202753

To link to this article: https://doi.org/10.1080/02786826.2023.2202753

AEROSOL SCIENCE AND TECHNOLOGY
2023, VOL. 57, NO. 7, 633–644
https://doi.org/10.1080/02786826.2023.2202753

Understanding the influence of atomizing power on electronic cigarette aerosol size and inhalation dose estimation

Jinho Lee[a], Wei-Chung Su[a,b], and Inkyu Han[c]

[a]Department of Epidemiology, Human Genetics, and Environmental Sciences, School of Public Health, University of Texas Health Science Center at Houston, Houston, Texas, USA; [b]Southwest Center for Occupational and Environmental Health (SWCOEH), School of Public Health, University of Texas Health Science Center at Houston, Houston, Texas, USA; [c]Department of Epidemiology and Biostatistics, Temple University College of Public Health, Philadelphia, Pennsylvania, USA

ABSTRACT

Although many studies have estimated the inhalation dose of aerosols emitted from electronic cigarettes (e-cigs), the association between the atomizing power and inhalation dose of e-cig aerosols has not been fully examined. The aim of this study was to determine the mass and inhalation doses of e-cig aerosols and their association with the atomizing power of vaping devices. Size-segregated aerosol masses were collected using an 11-stage cascade impactor and the deposition dose in the human respiratory tract was estimated using the size-segregated aerosol mass. The results showed that an increase in atomizing power was positively associated with the amount of aerosol mass generated (p-value < 0.001). The mass median aerodynamic diameter and mass mean diameter of aerosol were 0.91 μm and 0.84 μm, respectively. The average deposition fractions of aerosols in the head airway, tracheobronchial region, and alveolar region were 67.2, 6.2, and 26.6%, respectively. In conclusion, vaping with a higher atomizing power increases the e-cig aerosol inhalation dose in the airway.

ARTICLE HISTORY
Received 21 November 2022
Accepted 24 March 2023

EDITOR
Mark Swihart

1. Introduction

In recent decades, the global use of electronic cigarettes (e-cigs) has rapidly grown and replaced the use of conventional tobacco smoke (Reitsma et al. 2021). In the United States e-cig sales increased more than two-fold from 2014 (7.7 million) to 2020 (17.1 million), and the prevalence of e-cig ever-use in the European Union also increased from 7.2% (2012) to 14.0% (2020) (Ali et al. 2020; European Commission 2015, 2021). Although there are few e-cig users in East Asian countries, the number of e-cig users in East Asian countries has doubled or tripled, from 0.5% (2015) to 0.9% (2018) in China and from 1.1% (2013) to 3.3% (2019) in Korea (Korea Centers for Disease Control and Prevention 2015, 2021; Zhao et al. 2020).

Vaping devices have also evolved over time. First-generation e-cigs (cig-a-like) were only able to vape with a specific flavor and predetermined atomizing power. Second-generation devices (clearomizers) were designed to vaper using various atomizing power settings. Third-generation e-cigs, the mod (modification) type, allow consumers to choose the flavor according to their preferences. Currently, lightweight fourth-generation e-cigs (pods) are simplified with stable nicotine delivery using a fixed wattage (Williams and Talbot 2019).

Although evidence suggests that aerosol emissions are lower from vaping than from conventional tobacco smoking (Lampos et al. 2019; Martuzevicius et al. 2019; McAuley et al. 2012; Palmisani et al. 2019; Papaefstathiou et al. 2020; Ruprecht et al. 2017; Schripp et al. 2013), the inhalation dose of e-cig aerosols among vapers can be significantly higher due to the frequent use of vaping (Schoren, Hummel, and Vries 2017). Frequent use of e-cigs likely makes vapers inhale more e-cig aerosols than traditional tobacco smokers. Vaping in indoor environments is also increasing since the mode of e-cig consumption, referred to as 'stealth-vaping,' is discreet and difficult to detect, including in smoking-free zones (Jackson et al. 2020; Ramamurthi, Chau, and Jackler 2019; Reuters 2016; Yingst et al. 2019). This reduces

CONTACT Inkyu Han inkyu.han@temple.edu Department of Epidemiology and Biostatistics, Temple University College of Public Health, 1301 Cecile B. Moore Avenue, Ritter Annex #907 Philadelphia, PA 19122, USA.

Supplemental data for this article can be accessed online at https://doi.org/10.1080/02786826.2023.2202753.

people's awareness of the possible negative consequences of vaping. Further, the convenience of choosing the flavor and fragrances with less nuisance may act as a possible gateway to make people become active vapers (Khouja et al. 2020; National Academies of Sciences, Engineering, and Medicine 2018; Soneji et al. 2017).

Consequently, compared to traditional tobacco, smokers tend to use e-cigarettes more frequently, and the adjustable atomizer power encourages vapers to use e-cigarettes heavily, often at high power levels. Hence, an understanding of exposure to e-cig aerosols in vapers is necessary, especially the effect of flavor and atomizing power on exposure and inhalation dose. However, few studies have examined the effects of the atomizing power and flavor of vape liquid on the lung deposition of passive vapers.

Another knowledge gap lies in the aerosol collection method. While existing studies have estimated the deposition dose of e-cig aerosols using direct reading instruments (DRI) based on light scattering or particle mobility methods (Lechasseur et al. 2019; Son et al. 2020; Sosnowski and Kramek-Romanowska 2016; Zhou et al. 2021), the DRI method may not accurately estimate the deposition dose of e-cigarette aerosols because it relies on the indirect conversion of number concentrations in various aerosol sizes, using methods such as light scattering or particle mobility, which are dependent on assumptions about the less-precise density and shape of the aerosols. Therefore, an impactor sampling method has its strength because it collects aerosols that align with the physical and aerodynamic mass relevant to actual airway deposition.

However, the impactor method has only been employed in a few studies to characterize e-cigarette aerosol exposure among vapers (Sundahl, Berg, and Svensson 2017), and the effect of atomizing power on deposition dose has not been sufficiently determined. While several prior studies have examined the correlation between the number or estimated mass of e-cigarette aerosol and atomizing power or coil temperature under controlled conditions using exposure chambers (Schripp et al. 2013; Son et al. 2020; Zhao et al. 2016), none of these studies directly measured the aerosol mass, instead relying on assumed physical characteristics of the aerosols for estimation.

The objective of this study was to examine the effects of atomizing power and flavor of e-cigs on emissions of size-fractionated e-cig aerosol mass, as well as the estimated airway lung deposition dose from e-cig aerosols in an experimental chamber using a high-resolution cascade impactor.

2. Materials and methods

2.1. Materials and instruments

To generate e-cig aerosols and vapor, we used a third-generation e-cig device (Novo X; IVPS Technology Co., Shenzhen, China), which allows users to change their wattage (1 W to 25 W) and uses refillable cartridges. In this study, we purchased six popular flavored vape liquids (chocolate, melon, menthol, strawberry, grapefruit, and mango) from a local e-cig shop. Three liquids were nicotine-containing products, and the other three were nicotine-free (Table 1).

2.2. Experimental procedure

To estimate the deposition of e-cig aerosol mass in the respiratory system for passive vapers, we conducted a chamber study to characterize the size-fractionated e-cig aerosols generated from each flavored vape liquid. We used a stainless-steel chamber (61 cm (L) × 61 cm (W) × 61 cm (H)) equipped with an electric fan to ensure the homogeneous mixing of e-cig aerosols inside the chamber (Figure 1). The temperature and humidity of the laboratory and the chamber were maintained within the normal range (20 ± 5 °C, 50 ± 10 RH%).

A 100 mL syringe was used to draw e-cig aerosol from the vape device, and 100 ml of e-cig aerosol per puff was injected into the chamber every two minutes. To simulate the typical vaping topography of e-cig aerosols, the puff duration was 3 s for drawing 100 mL of e-cig aerosol/vapor. The 3 s period is recommended by the Cooperation Center for Scientific Research Relative to Tobacco (CORESTA) method 81 since 3 s is a representative average puff duration for normal vapers (CORESTA 2017). Prior studies about vaping topography reported an average puffing duration of 2.65 to 3.5 s (Behar, Hua, and Talbot 2015; Helen et al. 2016; Vansickel et al. 2018). Each puff was injected 30 times. The generation of e-cig aerosols for each flavored liquid was repeated using four output power settings (5, 10, 15, and 20 W). Therefore, a total

Table 1. The composition of the six E-cigarette liquids included in the study[a].

ID	Flavor	Nicotine Strength (mg/ml)	PG/VG Ratio	
			Vegetable Glycerol	Propylene Glycol
A	Chocolate	6.0	70.0	30.0
B	Melon	50	70.0	30.0
C	Menthol	6.0	50.0	50.0
D	Strawberry	Nicotine-free	65.0	35.0
E	Grapefruit	Nicotine-free	70.0	30.0
F	Mango	Nicotine-free	70.0	30.0

[a]The information in the table was filled in based on the label and safety data sheets of each product

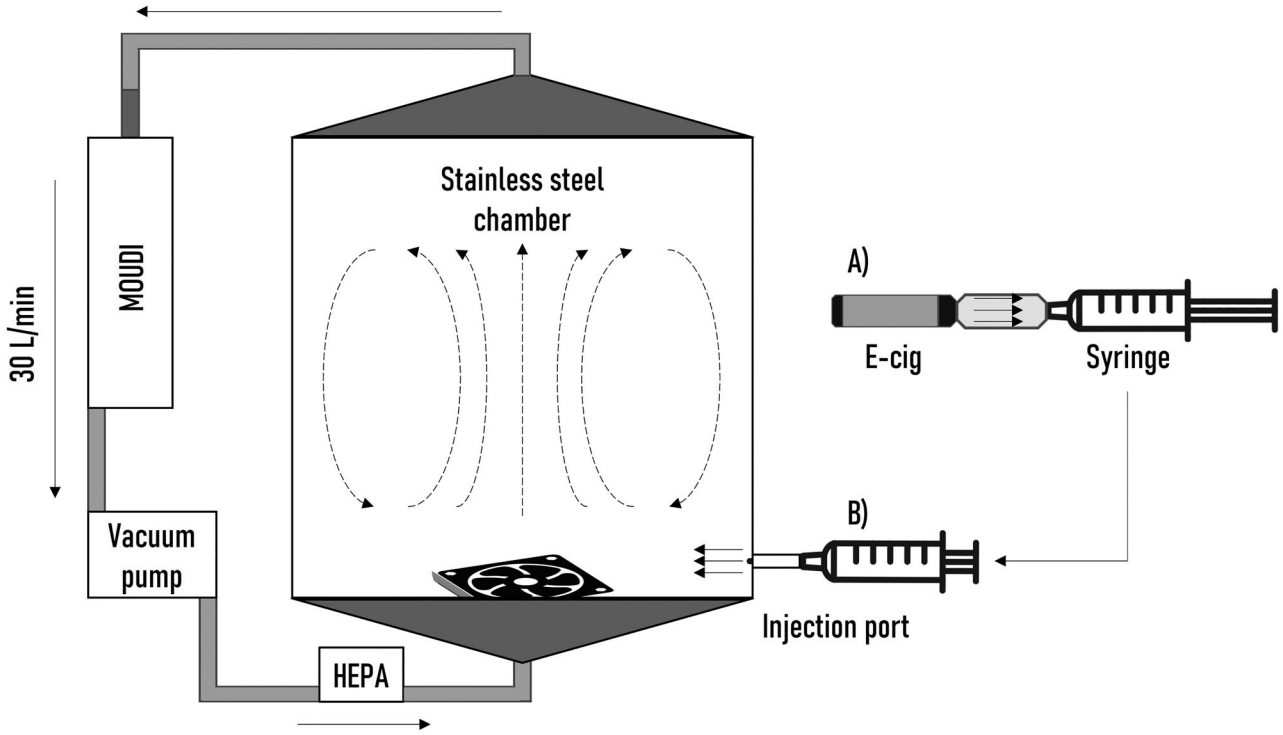

Figure 1. Schematic diagram of the experimental setup.

of 24 different experimental conditions (six flavors at four power settings) were used in this study.

E-cig aerosol injected into the chamber was sampled onto 37 mm Polytetrafluoroethylene (PTFE) membrane filters with 2.0 µm pore size (PALL Co., Port Washington, NY, USA) on an 11-stage Micro-orifice Uniform Deposit Impactor (MOUDI 110-R; MSP Co., Shoreview, MN, USA). MOUDI is a cascade impactor with aerosol cut points of 0.056, 0.1, 0.18, 0.32, 0.56, 1.0, 1.8, 3.2, 5.6, 10, and 18 μm at a flow rate of 30 L/min. After sample collection, the PTFE filter samples were immediately unloaded from the MOUDI and placed in individual Petri dishes. The filters were stabilized for at least 24 h in a room controlled at a constant temperature (~25 °C) and relative humidity (~50%). Subsequently, the masses of size-fractionated aerosols collected on PTFE filters were weighed using a microbalance (CAHN-32, ThermoFisher, Waltham, MA, USA) by subtracting the pre-experiment filter mass weight from the post-experiment filter mass weight.

2.3. Calculation and data analysis

2.3.1. Mass mean diameter and mass median diameter

We determined the mass mean diameter (MMD) and mass median aerodynamic diameter (MMAD) of e-cig aerosols based on size-fractionated aerosol mass weights. Equation (1) was used to calculate the MMD (Hinds and Zhu 2022).

$$MMD(\mu m) = \sum\left(\frac{m_i}{M} d_i\right) \quad (1)$$

where m_i is the sampled mass (μg) per puff in the MOUDI stage i, d_i is the aerosol diameter (μm) in MOUDI stage i, and M is the total mass (μg) per puff sampled.

The MMAD was estimated by analyzing the distribution of the aerosol mass by diameter, specifically by determining the cutoff of each impactor stage. We used gravimetric analysis to obtain the cumulative aerosol mass by size and constructed a cumulative mass plot of the aerosol by size. After log-transforming the 11-point cumulative raw data and testing for normality, we fitted them to a standard sigmoid curve. Based on this curve, we identified the diameter at which half the mass was contributed by particles larger than the MMAD and half the mass was contributed by particles smaller than the MMAD (Hinds and Zhu 2022).

A summary of descriptive statistics includes the comparison of the size-segregated aerosol concentrations by both power (different wattages) of the device and various flavors and the percentage of e-cig mass by both different size bins and flavors. The total masses of e-cig aerosol by both different wattages and flavors were compared using the Kruskal-Wallis test.

Similarly, the differences in mass and size distribution between nicotine-containing and nicotine-free liquids were examined using the Mann-Whitney U test, and Spearman's correlation analysis was used to test for correlations between the size of the aerosols (MMD and MMAD) and the atomizing power. All statistical analyses were conducted using the R software (V. 4.1.2; R Foundation, Vienna, Austria).

2.3.2. Respiratory deposition dose

Second, we estimated the deposition dose in the respiratory tract (Equation (2)).

$$Lung\ Deposition\ Dose(\mu g/puff) = \sum(m_i * f_{i,j}) \quad (2)$$

where m_i is the arithmetic mean of sampled mass (μg) per puff in the MOUDI stage i, $f_{i,j}$ is the deposition fraction of aerosol in the size range of MOUDI stage i, and the respiratory region j (j = head, tracheobronchial, and alveolar regions).

The lung deposition model of the International Commission on Radiological Protection (ICRP) was used for the deposition fraction (International Commission on Radiation Protection 1994).

3. Results

3.1. MMAD, MMD, and total mass by power and flavor

The MMAD, MMD, and aerosol mass by the atomizing power and aerosol size were summarized in Table 2. When estimating the MMAD, the data from each subgroup were consistent with the cumulative plots fitted to the model (p-value < 0.001, $R^2 > 0.98$). The MMAD of aerosols ranged from 0.40 to 0.84 µm, and the MMD of the aerosol ranged from 0.58 to 1.22 µm. At four levels of power (5, 10, 15, and 20 W), the overall MMADs were 0.54 ± 0.05, 0.54 ± 0.09, 0.57 ± 0.07, and 0.73 ± 0.09 µm, respectively. Similarly, the overall MMDs were 0.90 ± 0.10 µm for 5 W, 0.76 ± 0.12 µm for 10 W, 0.79 ± 0.08 µm for 15 W, and 1.12 ± 0.19 µm for 20 W (Table 2). The mass median diameter of the e-cig aerosol showed a positive correlation with the four atomizer power levels, but mass mean diameters did not show a positive correlation with the four atomizer power levels (p-value: 0.005 and 0.13, respectively). Given the small sample size in each group, not all log-transformed data from the subgroups demonstrated normality as determined by the Shapiro-Wilk test (p-value < 0.05), and the variances of the subgroup data were inconsistent. Therefore, we utilized the Kruskal-Wallis test to compare the groups. The results of the Kruskal-Wallis test indicated a significant difference in the MMAD and MMD between different power levels (p-value: 0.02 and 0.01, respectively). The *post hoc* test showed that the MMAD with 20 W atomization power was significantly higher than that with 5, 10, and 15 W (p-values: 0.03, 0.03, and 0.03, respectively). The MMD with 20 W atomization power was significantly higher than that with 10 W and 15 W (p-values: 0.03 and 0.03, respectively).

Furthermore, the total mass per puff of e-cig aerosol varied from 55.5 to 844.9 µg for all data

Table 2. Size-fractionated aerosol mass per puff.

Flavor	Power (Watts)	Mass per Puff (μg)	Impactor Cutoff (μm)											MMAD (μm)	MMD (μm)
			0.056	0.10	0.18	0.32	0.56	1.0	1.8	3.2	5.6	10	18		
Chocolate	5	117.0	0.1%	0.2%	2.0%	8.5%	50.4%	29.8%	7.5%	1.2%	0.1%	0.1%	0.1%	0.52	0.81
	10	372.3	0.0%	0.1%	1.8%	8.6%	20.4%	57.8%	10.3%	0.8%	0.0%	0.0%	0.0%	0.68	0.95
	15	299.8	0.1%	0.2%	6.8%	16.4%	35.9%	37.1%	3.2%	0.2%	0.0%	0.0%	0.1%	0.51	0.71
	20	269.4	0.2%	0.4%	3.0%	7.2%	37.8%	39.7%	10.1%	1.5%	0.1%	0.1%	0.0%	0.58	0.88
Melon	5	153.2	0.3%	0.1%	2.5%	10.5%	50.7%	27.0%	7.2%	1.2%	0.0%	0.2%	0.2%	0.50	0.83
	10	200.1	0.1%	0.2%	5.0%	13.5%	34.6%	42.0%	4.5%	0.1%	0.0%	0.0%	0.0%	0.54	0.76
	15	557.1	0.2%	0.0%	1.8%	8.2%	24.7%	55.3%	9.1%	0.7%	0.1%	0.0%	0.0%	0.66	0.91
	20	423.3	0.0%	0.0%	1.4%	6.3%	19.8%	51.1%	18.2%	3.1%	0.0%	0.0%	0.0%	0.76	1.08
Menthol	5	117.3	0.0%	21.7%	1.3%	6.8%	36.0%	20.7%	7.7%	3.0%	2.5%	0.1%	0.1%	0.46	0.86
	10	151.1	0.1%	0.1%	1.8%	8.3%	53.8%	32.3%	3.4%	0.1%	0.1%	0.0%	0.1%	0.51	0.74
	15	229.3	0.2%	0.2%	4.6%	14.7%	36.6%	39.2%	4.3%	0.3%	0.0%	0.0%	0.0%	0.53	0.74
	20	484.8	0.0%	2.4%	3.8%	6.5%	25.0%	44.0%	14.8%	3.2%	0.2%	0.0%	0.1%	0.68	1.00
Strawberry	5	163.8	0.4%	0.1%	2.4%	7.3%	39.0%	33.3%	11.4%	2.1%	3.8%	0.1%	0.1%	0.59	1.09
	10	229.0	0.0%	0.3%	9.8%	20.3%	35.4%	30.5%	3.5%	0.2%	0.0%	0.0%	0.0%	0.47	0.66
	15	503.5	0.0%	0.1%	4.0%	12.7%	17.9%	55.8%	8.7%	0.8%	0.0%	0.0%	0.0%	0.65	0.89
	20	465.3	0.0%	0.0%	2.7%	7.9%	22.2%	44.9%	17.6%	4.4%	0.1%	0.0%	0.0%	0.73	1.08
Grapefruit	5	349.2	0.0%	0.0%	1.3%	8.2%	38.0%	37.1%	12.1%	3.1%	0.1%	0.0%	0.0%	0.59	0.95
	10	280.1	0.0%	0.0%	1.3%	7.5%	34.5%	48.5%	7.0%	0.9%	0.1%	0.0%	0.1%	0.61	0.88
	15	155.6	1.5%	0.1%	3.4%	14.2%	44.3%	34.2%	1.9%	0.0%	0.3%	0.0%	0.0%	0.49	0.70
	20	844.9	0.1%	0.0%	0.7%	3.8%	19.3%	48.3%	22.3%	5.2%	0.1%	0.2%	0.0%	0.81	1.20
Mango	5	406.4	0.0%	0.1%	2.4%	9.3%	32.9%	46.7%	7.6%	0.9%	0.0%	0.0%	0.1%	0.60	0.86
	10	55.5	0.3%	2.0%	12.7%	13.4%	54.6%	16.4%	0.0%	0.3%	0.0%	0.0%	0.2%	0.40	0.58
	15	346.6	0.0%	0.1%	4.0%	12.8%	35.1%	42.9%	4.8%	0.3%	0.0%	0.0%	0.0%	0.55	0.77
	20	567.0	0.1%	0.0%	2.4%	6.8%	20.7%	34.4%	18.8%	12.3%	4.4%	0.1%	0.0%	0.84	1.48

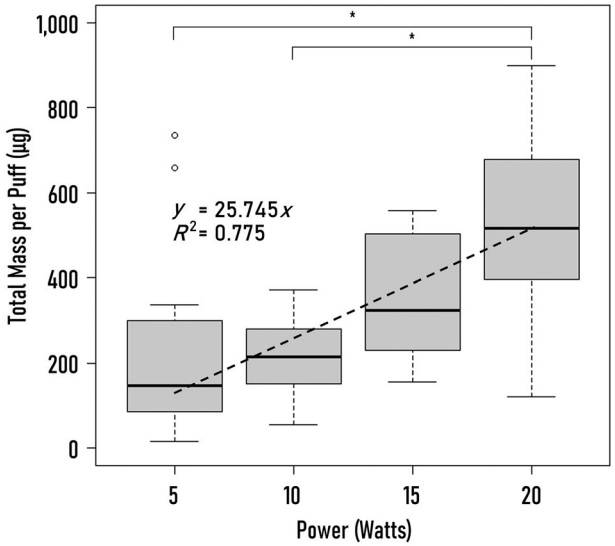

Figure 2. Total mass of E-cig aerosol per puff by the power of the device.
The lines within the boxes are medians, the bottom and top of the box mean 25th and 75th percentiles, respectively, and the lower and upper bars on whiskers are 10th and 90th percentiles, respectively (*: p-value < 0.05).

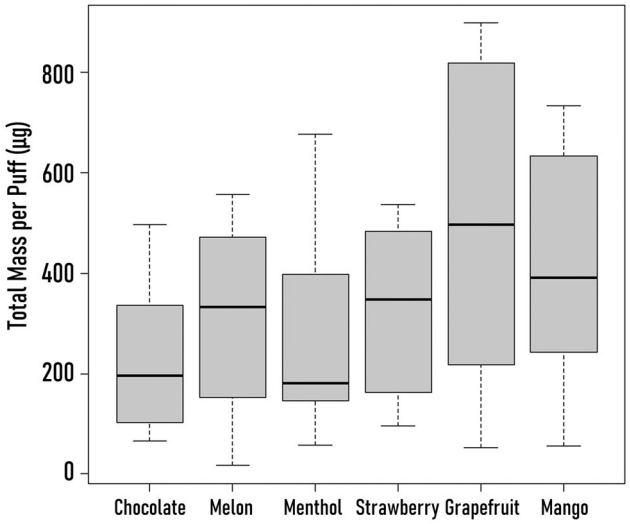

Figure 3. Total mass of E-cig aerosol per puff by flavor.
The lines within the boxes are medians, the bottom and top of the box mean 25th and 75th percentiles, respectively, and the lower and upper bars on whiskers are 10th and 90th percentiles, respectively.

(mean ± SD: 322.6 ± 181.7 µg/puff; Table 2). Similar to MMAD and MMD analyses, We utilized the Kruskal-Wallis test to compare the groups because the sample size in each subgroup (wattage and flavor) was small and not all of the subgroup data met the normality assumptions of the Shapiro-Wilk test (p-value $<$ 0.05). The means of the total mass of aerosol per puff at 5, 10, 15, and 20 W were 217.8 ± 200.6, 214.7 ± 99.1, 348.7 ± 155.8, and 509.1 ± 220.3 µg, respectively (Figure 2). There was a statistically significant difference in the total mass of e-cigarette aerosol across the four atomization power settings (p-value: $<$0.001). The *post hoc* test showed that the means of total aerosol mass significantly differed between 5 and 20 W and between 10 and 20 W (p-value: $<$0.001 and 0.05, respectively). Furthermore, the simple linear regression model showed a significant positive association between atomization power and the total mass of aerosol (p-value: $<$0.001), and the R^2 was 0.775.

However, the total mass of e-cig aerosols did not differ significantly among the six flavors (Figure 3). The mean total aerosol masses per puff for chocolate, melon, menthol, strawberry, grapefruit, and mango flavor were 228.9 ± 150.4, 310.8 ± 193.7, 273.3 ± 223.3, 327.5 ± 164.1, 502.3 ± 313.5, and 415.3 ± 238.3 µg, respectively ($p = 0.35$).

3.2. Size distribution of e-cig aerosol

The total aerosol mass concentrations were primarily attributed to the size cutoff between 0.56 and 1.0 µm, ranging from 68.5 to 75.4% (Figure 4). The log-transformed aerosol mass distribution was unimodal and bell-shaped for all six flavors. The mean mass diameter of each flavor (chocolate, melon, menthol, strawberry, grapefruit, and mango) was 0.84, 0.90, 0.84, 0.93, 0.93, and 0.92 µm, respectively.

Overall, the size of the e-cig aerosol with the highest weight increased from 0.56 to 1.0 µm, with increasing atomization power (Table 2). With the exception of mango, the mass-dominant size of the aerosol increased with increasing atomization power. However, there was no clear point at which the mass-dominant size of e-cig aerosol changed from 10 W to 20 W. More details on the size distribution of aerosol mass by flavor and power are provided in Figure S1.

3.3. Deposited dose of e-cig aerosol

We calculated the deposited dose per puff of e-cig aerosols using the ICRP lung deposition model (Table 3). The estimated deposited dose of e-cig aerosols with a size of between 0.56 and 1.8 µm was 75.8 ± 2.4% of the total aerosol mass in the respiratory tract. While the peak size ranges of the total mass of aerosol emitted from e-cigs (measured aerosol mass in the chamber) were between 0.56 and 1.0 µm, the particle size range primarily deposited in the respiratory tract was larger (1.0 to 1.8 µm).

Among the three human respiratory regions, the overall proportion of deposited dose per puff in the head airway was highest (67.2 ± 1.3%), followed by the alveolar region (26.6 ± 1.3%) and tracheobronchial

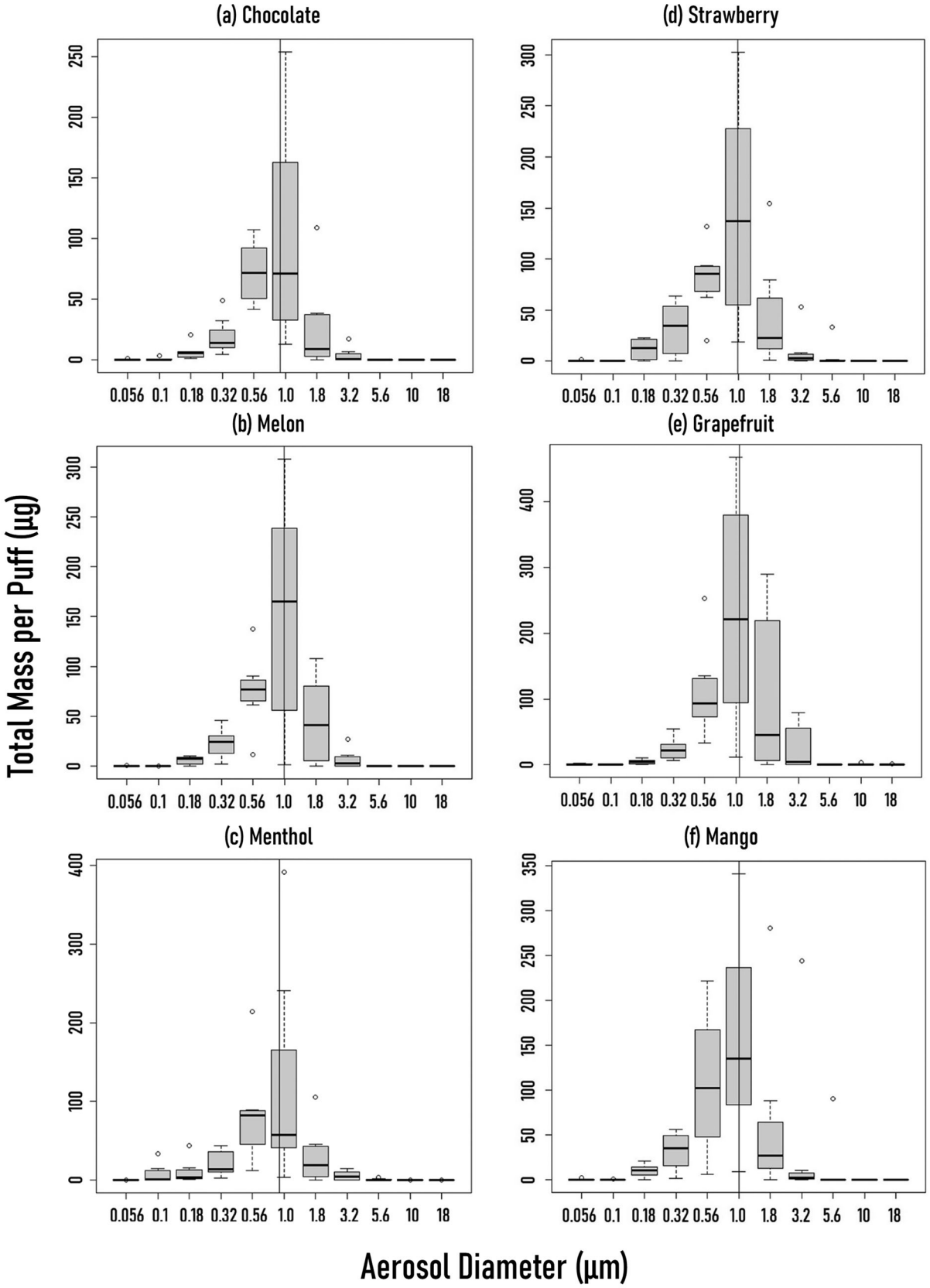

Figure 4. Total mass per puff by MOUDI Stage.
The X-axis (cut size) is represented in a log-transformed scale. Values shown are medians (line within box), 25th and 75th percentiles (bottom and top of the box, respectively), 10th and 90th percentiles (lower and upper bars on whiskers, respectively), and the solid vertical line is the mass mean diameter.

Table 3. Deposited dose of E-cigarette aerosol per puff (μg).

		Impactor Cutoff (μm)										
Flavor	Region	0.056	0.10	0.18	0.32	0.56	1.0	1.8	3.2	5.6	10	18
Chocolate	Head	0.012	0.019	0.175	1.065	9.226	34.09	16.17	3.060	0.089	0.083	0.060
	TB	0.022	0.024	0.076	0.105	0.686	3.247	1.576	0.236	0.004	0.002	>0.001
	Alveolar	0.102	0.128	0.508	1.318	6.886	14.55	3.657	0.359	0.005	0.002	0.001
Melon	Head	0.008	0.003	0.163	1.320	10.13	53.67	29.53	6.202	0.128	0.044	0.037
	TB	0.014	0.003	0.071	0.130	0.753	5.111	2.878	0.479	0.006	0.001	>0.001
	Alveolar	0.065	0.018	0.471	1.634	7.561	22.90	6.679	0.729	0.007	0.001	>0.001
Menthol	Head	0.003	0.105	0.314	1.235	11.45	42.18	20.23	4.794	0.567	0.088	0.112
	TB	0.006	0.131	0.137	0.122	0.851	4.018	1.971	0.370	0.026	0.002	0.001
	Alveolar	0.026	0.701	0.910	1.529	8.543	18.00	4.574	0.563	0.032	0.002	0.001
Strawberry	Head	0.004	0.006	0.335	1.883	10.64	50.79	29.67	9.065	1.621	0.068	0.056
	TB	0.008	0.007	0.146	0.185	0.791	4.838	2.891	0.700	0.074	0.001	>0.001
	Alveolar	0.036	0.039	0.970	2.331	7.939	21.68	6.710	1.065	0.092	0.002	>0.001
Grapefruit	Head	0.031	0.005	0.112	1.243	14.44	75.48	62.43	20.74	0.400	0.723	0.178
	TB	0.055	0.006	0.049	0.122	1.074	7.189	6.084	1.601	0.018	0.014	0.001
	Alveolar	0.259	0.032	0.324	1.539	10.78	32.21	14.12	2.436	0.023	0.017	0.001
Mango	Head	0.005	0.008	0.256	1.547	13.11	52.30	34.67	13.68	0.420	0.161	0.149
	TB	0.009	0.011	0.111	0.152	0.975	4.981	3.379	1.056	0.019	0.003	0.001
	Alveolar	0.043	0.056	0.742	1.915	9.787	22.32	7.841	1.607	0.024	0.004	0.001

region (6.2 ± 0.1%) The proportion particles with a sub-micrometer diameter ($\leq$ 1.0 µm) in the head airway, tracheobronchial region, and alveolar region were 62.2 ± 6.1%, 62.6 ± 6.0%, and 80.8 ± 4.2%, respectively. More details on the estimated deposited dose by the region of deposition, flavor, power, and aerosol size are provided in Table S1.

4. Discussion

This study examined the effects of aerosol atomization power on exposure to the total mass of e-cig aerosols, size-fractionated mass, and estimated deposited dose in the human respiratory system in an exposure chamber.

4.1. MMAD, MMD, and total mass by power and flavor

The results of this study showed a positive correlation between the total aerosol mass per puff and an increase in the atomization power (wattage) of the e-cigarette device. Notably, the total aerosol mass was significantly higher when the vape liquid did not contain nicotine, and the majority of the aerosol mass was comprised of particles smaller than 1.0 µm. Our analysis examined several factors influencing aerosol emission from e-cigarettes, including unit puff volume, atomization power, and ingredient characteristics. While the lowest values from the literature were comparable with the results in this study (0.003 ± 0.002 mg/mL-puff, 0.001 to 0.008 mg/mL-puff), the total mass per puff volume in existing studies varied widely; 0.003 to 0.133 mg/mL-puff (Floyd et al. 2018; Ingebrethsen, Cole, and Alderman 2012; Kane and Li 2021; Pourchez et al. 2018; Prévôt et al. 2017). The range of total aerosol mass per unit puff and volume did not differ significantly across prior studies using normalized aerosol mass by the number of puffs and puff volume. For instance, the normalized aerosol mass using a DRI instrument ranged from 0.003 to 0.133 mg/mL-puff (Floyd et al. 2018), and that using impactor sampling methods ranged from 0.004 to 0.118 mg/mL-puff (Ingebrethsen, Cole, and Alderman 2012 (0.025 to 0.105 mg/mL-puff); Kane and Li 2021 (0.033 to 0.118 mg/mL-puff); Pourchez et al. 2018 (0.004 to 0.023 mg/mL-puff); Prévôt et al. 2017 (0.065 to 0.070 mg/mL-puff)). The relatively low emission rates we observed in this study may have resulted from different study designs and experimental methods. For instance, previous studies measured aerosol exposure to active vapers by determining the total mass per puff of e-cig aerosols collected in a syringe and directly introducing them to a sampling medium. In contrast, our study examined exposure by collecting the generated e-cig aerosols in a syringe and introducing aerosols into an exposure chamber with clean air. Thus, the total mass per unit puff volume in our study might be lower because of dilution with fresh air.

4.2. Size distribution of e-cig aerosol

The particle size distribution and MMAD in this study were comparable with those observed in previous studies that reported that the mode of e-cig aerosols was smaller than 1 µm (Kane and Li 2021; Pourchez et al. 2018; Pratte, Cosandey, and Goujon-Ginglinger 2016). For example, the MMAD in this study ranged from 0.58-1.04 µm, and our results agree with previous studies using a cascade impactor

method that reported the range of MMAD from 0.70 µm to 1.3 µm (Kane and Li 2021; Pourchez et al. 2018; Prévôt et al. 2017; Werley et al. 2016). These results confirmed that the aerosols from e-cigs were mostly condensed.

To investigate how atomization power impacts the physical properties of e-cigarette aerosol, we adjusted the atomizer's power between 5 and 20 W in 5 W increments. Previous research has shown that raising the atomization power increases the temperature of the heating coil, leading to the production of more aerosol (Floyd et al. 2018; Gillman et al. 2016; Pourchez et al. 2018; Son et al. 2020). However, the relationship between increasing power and MMAD (mass median aerodynamic diameter) produced inconsistent findings. While some studies have reported an increase in MMAD with an increase in wattage (Floyd et al. 2018; Pourchez et al. 2018), others have not found this association (Son et al. 2020).

This study demonstrated that increasing the atomization power from 5 W to 20 W led to a rise in the amount of aerosol produced, and there was a trend toward an increase in MMAD as the wattage increased. The growth of aerosol mass sizes between $0.32 - 1.0$ µm was strongly associated with the high voltage of atomization power. In contrast, the increase of aerosol mass by increasing atomization power was not observed for the sizes smaller than 0.32 µm or greater than 1.0 µm. These results suggest that inhaled e-cig aerosols are likely to be deposited in the lower airways and alveoli.

4.3. Deposited dose of e-cig aerosol

Along with the effect of atomization power on the physical characteristics of e-cig aerosols, the estimation of aerosol lung deposition dose is one of the significant findings of this study. The inhaled aerosol dose per puff was the highest in the head airway, followed by the alveolar and tracheobronchial regions.

Applying the semi-empirical aerosol respiratory deposition model may have limitations since the current ICRP and MPPD deposition models are dedicated to solid particles (International Commission on Radiation Protection 1994; Miller et al. 2016). Despite this, the use of ICRP and MPPD models is a feasible approach to estimating lung deposition of e-cig aerosols due to the lack of an aerosol deposition estimation model for liquid particles and vapors. Prior studies have estimated the respiratory deposition of e-cig aerosols by measuring the size and mass of the aerosols using DRI, such as a scanning mobility particle sizer or other spectrometers (Belka et al. 2017; Floyd et al. 2018; Ingebrethsen, Cole, and Alderman 2012; Lerner et al. 2015; Mikheev et al. 2016; Papaefstathiou et al. 2020; Pratte, Cosandey, and Goujon-Ginglinger 2016). Although these real-time measurement methods effectively estimate the mass and size of ultrafine particles, they are indirect methods for estimating mass and size distributions by converting particle count concentrations to mass concentrations. The conversion is heavily influenced by several assumptions, such as particle shape and density, which may cause large uncertainties and errors. Because optical techniques are unable to detect particles smaller than 50-100 nm and are susceptible to sizing errors due to variations in particle shape and refractive index, most ultrafine particle detectors use a condensation particle counter (CPC) with a differential mobility analyzer to detect the size and number of ultrafine particles. However, the CPC measures supersaturated and enlarged particles, and the non-uniform supersaturation makes the cutoff of the measurement less sharp. In converting the size-based particle number concentration to the mass, most models usually assume that the particles are spherical. Hence, the calculated mass is also sensitive to variations in the particle shape. Additionally, the particle density must be determined in most cases, whereas the density of particulates is set arbitrarily (e.g., assuming that the density of particles is the same regardless of the size range). However, the relationship between aerosol density and size in e-cigarettes is not yet clearly understood. As a result, previous studies calculated the respiratory deposited mass of e-cigarette aerosol using DRI (deposition-related inhalation) and focused on the mass deposition fraction solely based on aerosol size (Lechasseur et al. 2019; Sosnowski and Kramek-Romanowska 2016), or assumed that the aerosol would have particular value in density that was estimated from the e-cig liquid that is not vaporized (Son et al. 2020). Furthermore, this method needs an assumption that every size of e-cig aerosol has the same density. Given the above limitations, the count-based mass conversion data may have discrepancies in estimating the lung deposition dose of the aerosol mass because the count-based data can be complementary to the directly measured mass of aerosols using a cascade impactor.

Although using a cascade impactor to characterize e-cig aerosol mass is considered the "standard method," to our knowledge, only our study and another study by Sundahl, Berg, and Svensson (2017) directly

measured and estimated the lung deposition of the e-cig-generated aerosol using a cascade impactor. For instance, Sundahl, Berg, and Svensson (2017) used a 7-stage cascade impactor to estimate e-cig aerosol lung deposition based on a multiple-path particle dosimetry model. In our study, we used an 11-stage impactor with a more accurate aerosol diameter resolution, including nano sizes. We also evaluated the passive vaper's inhaled dose using an exposure chamber, while Sundahl, Berg, and Svensson (2017) focused on the active vaper's exposure by directly injecting the e-cig aerosol into the impactor.

Furthermore, we determined the association between atomization power and the physical characteristics of e-cig aerosols based on their size. Even though current and widely used devices easily adjust the generation rate of e-cig vapor by changing its atomization power, few studies have systematically examined the effect of power on aerosol mass emission. Pourchez et al. (2018) determined the effect of atomization power on aerosol mass using a low-pressure impactor. However, the authors sampled aerosols using a puff volume of 2,000 mL, which is unrealistic for e-cig users in real-world environments. In this study, the emission of e-cig aerosol was generated at 100 mL/puff as a representative vaping topology of the established e-cig user (Lee et al. 2018; Mikheev et al. 2020; Lopez et al. 2016).

Despite its strength, this study has several limitations. Although the higher atomization power led to an increase in e-cig aerosol generation, the relationship between the generated e-cig aerosol and atomization power was not entirely determined because of the relatively small sample size ($n = 3$ for each setting) with four levels of atomization power. Particle loss due to evaporation may occur during sampling in the exposure chamber, although most aerosols generated from the e-cig liquid primarily consist of delivery solvents such as propylene glycol (PG) and vegetable glycerol (VG), which are semi-volatile at room temperature and pressure. Volatile organic chemicals (VOCs), such as hydrocarbons, aldehydes, alcohols, and aromatic hydrocarbons, are also emitted during e-cig use (Lee et al. 2017; Omaiye et al. 2019; Papaefstathiou et al. 2020). Our study may not reflect the weight of these volatile organic compounds in the air because the volatile compounds generated from e-cigs can easily evaporate during sampling. However, previous studies have reported that the mass of VOCs in e-cig aerosols is the least compared to major ingredients such as PG and glycerol. The estimated total mass of these volatile compounds is less than 3% of the total mass of aerosols (Canistro et al. 2017). Thus, the characterization of e-cig aerosols is unlikely to be underestimated, despite the potential small loss of VOCs due to vaporization during sampling. Although we maintained good experimental control throughout the study, we did not measure the temperature and relative humidity inside the chamber. However, we expect the temperature and humidity to be similar to the HVAC-controlled temperature and humidity of the laboratory ($20 \pm 5\,^{\circ}C$, 50 ± 10 RH%). It is worth noting that the temperature and humidity of inhaled air before reaching the pharynx typically reach higher levels (31-34 °C, 90 RH%, Issakhov and Zhandaulet 2019). Therefore, the relatively lower temperature and humidity inside the chamber may have reduced the size and amount of e-cigarette aerosol produced (Son et al. 2020). However, the exact impact of temperature and humidity on the study's results is difficult to ascertain since there is a lack of research on the association between e-cigarette aerosol, temperature, and humidity. Despite this uncertainty, all experiments were conducted under the same environmental condition. Thus, the systematic bias might be relatively small across all experiments.

One of the limitations of this study is the inconsistency of the PG/VG ratio used in the e-cigarette liquids. Previous research has suggested that an increase in PG proportion contributes to the high volatility of e-cigarette liquid. In our study, the Menthol flavor had a relatively higher PG/VG ratio (50:50) compared to the other flavors (30:70 and 35:65), but we found no significant differences in total mass, MMAD, and MMD between the Menthol flavor and the others at the same atomization power. Although determining the impact of the PG/VG ratio on e-cigarette particle mass is important, it poses a challenge due to inconclusive findings from prior research on the link between PG/VG ratio and aerosol mass and size distribution. Several studies have examined the relationship between PG/VG ratios and e-cigarette particle mass. Some have found that higher ratios of PG/VG were associated with increased total e-cigarette particle mass per puff (El-Hellani et al. 2018; Talih et al. 2020). Conversely, lower ratios of PG/VG were linked to reduced total e-cigarette particle mass per puff in other studies (Baassiri et al. 2017; Li et al. 2021). In contrast, some research has found that lower PG/VG ratios were associated with increased overall aerosol mass emission (Dibaji et al. 2022; Pourchez et al. 2018). Regarding particle size, some studies have reported that e-liquids with higher PG proportions generate smaller particles, while others have found that higher PG/VG ratios result in bigger

particles (Stefaniak et al. 2022). Thus, further studies are required to determine whether the PG/VG ratio significantly affects aerosol mass and size distribution.

To better understand the inhalation exposure to e-cigarettes, it is necessary to estimate the physical characteristics of the aerosols produced by e-cigarettes and how they deposit in the respiratory system of vapers. Additionally, it is important to determine the association between aerosol mass and atomizing power. Because this study used an impactor that can only cover two size bins of ultrafine particles (56 nm and 100 nm), an impactor with a higher resolution can provide more precise results for the size distribution of ultrafine e-cig aerosols. Additionally, to understand aerosol characteristics in real-world environments, experimental conditions that can represent a 'typical' indoor environment and realistic vaping conditions need to be examined. In this study, we applied a chamber experience model to mimic the exhaled e-cigarette aerosol and vapor exposure to passive smokers in near-distance indoor environments. However, there may be a difference in e-cigarette aerosol deposition in the active vaper's respiratory tract and the test syringe that we used. Moreover, the exposure to e-cigarette vapor may differ from the exposure in the typical room that has a relatively larger volume than the exposure chamber. Furthermore, considering the total exposure to e-cig emissions, the exposure assessment of both gas and liquid phases needs to be assessed in future studies.

5. Conclusion

In our study, we found that increasing the atomizing power of e-cigarettes resulted in a higher estimated inhalation dose of e-cig aerosols, and these aerosols are mainly deposited in the head airways and alveolar regions of the respiratory system. Vapers who use e-cigarettes with higher atomizing power may be exposed to higher levels of e-cig emissions, highlighting the need to promote awareness of this potential risk. Moreover, future research on the health effects associated with both active and passive exposure to e-cigarette emissions is necessary.

Disclosure statement

The authors report there are no competing interests to declare.

Funding

This research was supported, in part, by the National Institute Environmental Health Sciences (NIEHS) under Grant (R21ES031795); and by a Pilot award from Gulf Coast Center for Precision Environmental Health (GC-CPEH), an NIEHS P30 Environmental Health Sciences Core Center under Grant (P30ES030285) at Baylor College of Medicine.

ORCID

Jinho Lee http://orcid.org/0000-0003-1660-3597
Wei-Chung Su http://orcid.org/0000-0002-7962-4021
Inkyu Han http://orcid.org/0000-0002-6147-7190

References

Ali, F. R. M., M. C. Diaz, D. Vallone, M. A. Tynan, J. Cordova, E. L. Seaman, K. F. Trivers, B. A. Schillo, B. Talley, and B. A. King. 2020. E-cigarette unit sales, by product and flavor type—United States, 2014–2020. *MMWR. Morb. Mortal. Wkly. Rep.* 69 (37):1313–8. doi: 10.15585/mmwr.mm6937e2.

Baassiri, M., S. Talih, R. Salman, N. Karaoghlanian, R. Saleh, R. El Hage, N. Saliba, and A. Shihadeh. 2017. Clouds and "throat hit": Effects of liquid composition on nicotine emissions and physical characteristics of electronic cigarette aerosols. *Aerosol Sci. Technol.* 51 (11): 1231–9. doi:10.1080/02786826.2017.1341040.

Behar, R. Z., M. Hua, and P. Talbot. 2015. Puffing topography and nicotine intake of electronic cigarette users. *PLoS One.* 10 (2):e0117222. doi:10.1371/journal.pone.0117222.

Belka, M., F. Lizal, J. Jedelsky, M. Jicha, and J. Pospisil. 2017. Measurement of an electronic cigarette aerosol size distribution during a puff. *EPJ Web Conf.* 143:02006. doi: 10.1051/epjconf/201714302006.

Canistro, D., F. Vivarelli, S. Cirillo, C. Babot Marquillas, A. Buschini, M. Lazzaretti, L. Marchi, V. Cardenia, M. T. Rodriguez-Estrada, M. Lodovici, et al. 2017. E-cigarettes induce toxicological effects that can raise the cancer risk. *Sci. Rep.* 7 (1):2028. doi:10.1038/s41598-017-02317-8.

CORESTA 2017. CORESTA recommended method N° 81. In *2015 collaborative study for determination of glycerin, propylene glycol, water and nicotine in collected aerosol of e-cigarettes*. Paris, France: CORESTA E-Cigarette Task Force.

Dibaji, S. A. R., B. Oktem, L. Williamson, J. DuMond, T. Cecil, J. P. Kim, S. Wickramasekara, M. Myers, and S. Guha. 2022. Characterization of aerosols generated by high-power electronic nicotine delivery systems (ENDS): Influence of atomizer, temperature and PG:VG ratios. *PLoS One.* 17 (12):e0279309. doi:10.1371/journal.pone.0279309.

El-Hellani, A., R. Salman, R. El-Hage, S. Talih, N. Malek, R. Baalbaki, … N. A. Saliba. 2018. Nicotine and carbonyl emissions from popular electronic cigarette products: Correlation to liquid composition and design characteristics. *Nicotine and Tobacco Research* 20 (2):215–23.

European Commission. 2015. *Eurobarometer 429: Attitudes of Europeans towards tobacco and electronic cigarettes*. Brussels, Belgium: European Union.

European Commission. 2021. *Eurobarometer 506: Attitudes of Europeans towards tobacco and electronic cigarettes*. Brussels, Belgium: European Union.

Floyd, E. L., L. Queimado, J. Wang, J. L. Regens, and D. L. Johnson. 2018. Electronic cigarette power affects count concentration and particle size distribution of vaping aerosol. *PLoS One.* 13 (12):e0210147. doi:10.1371/journal.pone.0210147.

Gillman, I. G., K. A. Kistler, E. W. Stewart, and A. R. Paolantonio. 2016. Effect of variable power levels on the yield of total aerosol mass and formation of aldehydes in e-cigarette aerosols. *Regul. Toxicol. Pharmacol.* 75:58–65. doi:10.1016/j.yrtph.2015.12.019.

Helen, G. S., K. C. Ross, D. A. Dempsey, C. M. Havel, P. Jacob, and N. L. Benowitz. 2016. Nicotine delivery and vaping behavior during ad libitum e-cigarette access. *Tob. Regul. Sci.* 2 (4):363–76. doi:10.18001/TRS.2.4.8.

Hinds, W. C., and Y. Zhu. 2022. *Aerosol technology: Properties, behavior, and measurement of airborne particles*. John Wiley & Sons: New York, NY, USA, ISBN 978-11-1949-404-1.

Ingebrethsen, B. J., S. K. Cole, and S. L. Alderman. 2012. Electronic cigarette aerosol particle size distribution measurements. *Inhal. Toxicol.* 24 (14):976–84. doi:10.3109/08958378.2012.744781.

International Commission on Radiation Protection. 1994. Human respiratory tract model for radiological protection. Publication 66. Ottawa, Canada: ICRP.

Issakhov, A., and Y. Zhandaulet. 2019. Numerical simulation of thermal pollution zones' formations in the water environment from the activities of the power plant. *Eng. Appl. Comput. Fluid Mech.* 13 (1):279–99. doi:10.1080/19942060.2019.1584126.

Jackson, A., G. Kong, R. Wu, M. E. Morean, D. R. Davis, D. R. Camenga, D. A. Cavallo, K. W. Bold, P. Simon, and S. Krishnan-Sarin. 2020. E-cigarette devices used on school grounds. *Addict. Behav.* 110:106516. doi:10.1016/j.addbeh.2020.106516.

Kane, D. B., and W. Li. 2021. Particle size measurement of electronic cigarette aerosol with a cascade impactor. *Aerosol Sci. Technol.* 55 (2):205–14. doi:10.1080/02786826.2020.1849536.

Khouja, J. N., S. F. Suddell, S. E. Peters, A. E. Taylor, and M. R. Munafò. 2020. Is e-cigarette use in non-smoking young adults associated with later smoking? A systematic review and meta-analysis. *Tob. Control.* 30 (1):8–15. doi:10.1136/tobaccocontrol-2019-055433.

Korea Centers for Disease Control and Prevention. 2015. Korea Health Statistics 2014. Korea National Health and Nutrition Examination Survey (KNHANES VI-2)

Korea Centers for Disease Control and Prevention. 2021. Korea Health Statistics 2019. Korea National Health and Nutrition Examination Survey (KNHANES VIll-1)

Lampos, S., E. Kostenidou, K. Farsalinos, Z. Zagoriti, A. Ntoukas, K. Dalamarinis, P. Savranakis, G. Lagoumintzis, and K. Poulas. 2019. Real-time assessment of e-cigarettes and conventional cigarettes emissions: Aerosol size distributions, mass and number concentrations. *Toxics* 7 (3):45. doi:10.3390/toxics7030045.

Lechasseur, A., S. Altmejd, N. Turgeon, G. Buonanno, L. Morawska, D. Brunet, C. Duchaine, and M. C. Morissette. 2019. Variations in coil temperature/power and e-liquid constituents change size and lung deposition of particles emitted by an electronic cigarette. *Physiol. Rep.* 7 (10):e14093. doi:10.14814/phy2.14093.

Lee, M. S., R. F. LeBouf, Y. S. Son, P. Koutrakis, and D. C. Christiani. 2017. Nicotine, aerosol particles, carbonyls and volatile organic compounds in tobacco-and menthol-flavored e-cigarettes. *Environ. Health* 16 (1):1–10. doi:10.1186/s12940-017-0249-x.

Lee, Y. O., J. M. Nonnemaker, B. Bradfield, E. C. Hensel, and R. J. Robinson. 2018. Examining daily electronic cigarette puff topography among established and nonestablished cigarette smokers in their natural environment. *Nicotine Tob. Res.* 20 (10):1283–8. doi:10.1093/ntr/ntx222.

Lerner, C. A., I. K. Sundar, R. M. Watson, A. Elder, R. Jones, D. Done, R. Kurtzman, D. J. Ossip, R. Robinson, S. McIntosh, et al. 2015. Environmental health hazards of e-cigarettes and their components: Oxidants and copper in e-cigarette aerosols. *Environ. Pollut.* 198:100–7. doi:10.1016/j.envpol.2014.12.033.

Li, Y., A. E. Burns, L. N. Tran, K. A. Abellar, M. Poindexter, X. Li, A. K. Madl, K. E. Pinkerton, and T. B. Nguyen. 2021. Impact of e-liquid composition, coil temperature, and puff topography on the aerosol chemistry of electronic cigarettes. *Chem. Res. Toxicol.* 34 (6):1640–54. doi:10.1021/acs.chemrestox.1c00070.

Lopez, A. A., M. M. Hiler, E. K. Soule, C. P. Ramôa, N. V. Karaoghlanian, T. Lipato, A. B. Breland, A. L. Shihadeh, and T. Eissenberg. 2016. Effects of electronic cigarette liquid nicotine concentration on plasma nicotine and puff topography in tobacco cigarette smokers: A preliminary report. *Nicotine Tob. Res.* 18 (5):720–3. doi:10.1093/ntr/ntv182.

Martuzevicius, D., T. Prasauskas, A. Setyan, G. O'Connell, X. Cahours, R. Julien, and S. Colard. 2019. Characterization of the spatial and temporal dispersion differences between exhaled e-cigarette mist and cigarette smoke. *Nicotine Tob. Res.* 21 (10):1371–7. doi:10.1093/ntr/nty121.

McAuley, T. R., P. K. Hopke, J. Zhao, and S. Babaian. 2012. Comparison of the effects of e-cigarette vapor and cigarette smoke on indoor air quality. *Inhal. Toxicol.* 24 (12):850–7. doi:10.3109/08958378.2012.724728.

Mikheev, V. B., M. C. Brinkman, C. A. Granville, S. M. Gordon, and P. I. Clark. 2016. Real-time measurement of electronic cigarette aerosol size distribution and metals content analysis. *Nicotine Tob. Res.* 18 (9):1895–902. doi:10.1093/ntr/ntw128.

Mikheev, V. B., S. S. Buehler, M. C. Brinkman, C. A. Granville, T. E. Lane, A. Ivanov, K. M. Cross, and P. I. Clark. 2020. The application of commercially available mobile cigarette topography devices for e-cigarette vaping behavior measurements. *Nicotine Tob. Res.* 22 (5):681–8. doi:10.1093/ntr/nty190.

Miller, F. J., B. Asgharian, J. D. Schroeter, and O. T. Price. 2016. Improvements and additions to the Multiple Path Particle Dosimetry model. *J. Aerosol Sci.* 99:14–26. doi:10.1016/j.jaerosci.2016.01.018.

National Academies of Sciences, Engineering, and Medicine. 2018. *Public health consequences of e-cigarettes*. Washington, DC, USA: National Academies of Sciences, Engineering, and Medicine.

Omaiye, E. E., K. J. McWhirter, W. Luo, P. A. Tierney, J. F. Pankow, and P. Talbot. 2019. High concentrations of flavor chemicals are present in electronic cigarette refill fluids. *Sci. Rep.* 9 (1):1–9. doi:10.1038/s41598-019-39550-2.

Palmisani, J., A. Di Gilio, L. Palmieri, C. Abenavoli, M. Famele, R. Draisci, and G. de Gennaro. 2019. Evaluation of second-hand exposure to electronic cigarette vaping under a real scenario: Measurements of ultrafine particle number concentration and size distribution and comparison with traditional tobacco smoke. *Toxics* 7 (4):59. doi:10.3390/toxics7040059.

Papaefstathiou, E., S. Bezantakos, M. Stylianou, G. Biskos, and A. Agapiou. 2020. Comparison of particle size distributions and volatile organic compounds exhaled by e-cigarette and cigarette users. *J. Aerosol Sci.* 141:105487. doi:10.1016/j.jaerosci.2019.105487.

Pourchez, J., S. Parisse, G. Sarry, S. Perinel-Ragey, J. M. Vergnon, A. Clotagatide, and N. Prévot. 2018. Impact of power level and refill liquid composition on the aerosol output and particle size distribution generated by a new-generation e-cigarette device. *Aerosol Sci. Technol.* 52 (4):359–69. doi:10.1080/02786826.2017.1422857.

Pratte, P., S. Cosandey, and C. Goujon-Ginglinger. 2016. A scattering methodology for droplet sizing of e-cigarette aerosols. *Inhal. Toxicol.* 28 (12):537–45. doi:10.1080/08958378.2016.1224956.

Prévôt, N., F. de Oliveira, S. Perinel-Ragey, T. Basset, J. M. Vergnon, and J. Pourchez. 2017. Nicotine delivery from the refill liquid to the aerosol via high-power e-cigarette device. *Sci. Rep.* 7 (1):2592. doi:10.1038/s41598-017-03008-0.

Ramamurthi, D., C. Chau, and R. K. Jackler. 2019. JUUL and other stealth vaporisers: Hiding the habit from parents and teachers. *Tob. Control* 28 (6):610–6. doi:10.1136/tobaccocontrol-2018-054455.

Reitsma, M. B., L. S. Flor, E. C. Mullany, V. Gupta, S. I. Hay, and E. Gakidou. 2021. Spatial, temporal, and demographic patterns in prevalence of smoking tobacco use and initiation among young people in 204 countries and territories, 1990–2019. *Lancet. Public Health.* 6 (7):e472–e481. doi:10.1016/S2468-2667(21)00102-X.

Reuters 2016. E-cigarette users view smoke-free areas as okay for vaping. Fortune. https://fortune.com/2016/09/22/ecigarette-smoke-free-areas-okay-vaping/

Ruprecht, A. A., C. De Marco, A. Saffari, P. Pozzi, R. Mazza, C. Veronese, G. Angellotti, E. Munarini, A. C. Ogliari, D. Westerdahl, et al. 2017. Environmental pollution and emission factors of electronic cigarettes, heat-not-burn tobacco products, and conventional cigarettes. *Aerosol Sci. Technol.* 51 (6):674–84. doi:10.1080/02786826.2017.1300231.

Schoren, C., K. Hummel, and H. Vries. 2017. Electronic cigarette use: Comparing smokers, vapers, and dual users on characteristics and motivational factors. *Tob. Prev. Cessation* 3 (April):8. doi:10.18332/tpc/69392.

Schripp, T., D. Markewitz, E. Uhde, and T. Salthammer. 2013. Does e-cigarette consumption cause passive vaping? *Indoor Air.* 23 (1):25–31. doi:10.1111/j.1600-0668.2012.00792.x.

Son, Y., G. Mainelis, C. Delnevo, O. A. Wackowski, S. Schwander, and Q. Meng. 2020. Investigating e-cigarette particle emissions and human airway depositions under various e-cigarette-use conditions. *Chem. Res. Toxicol.* 33 (2):343–52. doi:10.1021/acs.chemrestox.9b00243.

Soneji, S., J. L. Barrington-Trimis, T. A. Wills, A. M. Leventhal, J. B. Unger, L. A. Gibson, J. Yang, B. A. Primack, J. A. Andrews, R. A. Miech, et al. 2017. Association between initial use of e-cigarettes and subsequent cigarette smoking among adolescents and young adults: A systematic review and meta-analysis. *JAMA Pediatr.* 171 (8):788–97. doi:10.1001/jamapediatrics.2017.1488.

Sosnowski, T. R., and K. Kramek-Romanowska. 2016. Predicted deposition of e-cigarette aerosol in the human lungs. *J. Aerosol Med. Pulm. Drug Deliv.* 29 (3):299–309. doi:10.1089/jamp.2015.1268.

Stefaniak, A. B., A. C. Ranpara, M. A. Virji, and R. F. LeBouf. 2022. Influence of E-Liquid Humectants, Nicotine, and Flavorings on Aerosol Particle Size Distribution and Implications for Modeling Respiratory Deposition. *Front. Public Health* 10:782068. doi:10.3389/fpubh.2022.782068.

Sundahl, M., E. Berg, and M. Svensson. 2017. Aerodynamic particle size distribution and dynamic properties in aerosols from electronic cigarettes. *J. Aerosol Sci.* 103:141–50. doi:10.1016/j.jaerosci.2016.10.009.

Talih, S., R. Salman, R. El-Hage, N. Karaoghlanian, A. El-Hellani, N. Saliba, and A. Shihadeh. 2020. Effect of free-base and protonated nicotine on nicotine yield from electronic cigarettes with varying power and liquid vehicle. *Sci. Rep.* 10 (1):16263. doi:10.1038/s41598-020-73385-6.

Vansickel, A. R., J. S. Edmiston, Q. Liang, C. Duhon, C. Connell, D. Bennett, and M. Sarkar. 2018. Characterization of puff topography of a prototype electronic cigarette in adult exclusive cigarette smokers and adult exclusive electronic cigarette users. *Regul. Toxicol. Pharmacol.* 98:250–6. doi:10.1016/j.yrtph.2018.07.019.

Werley, M. S., J. H. Miller, IV, D. B. Kane, C. S. Tucker, W. J. McKinney, Jr, and M. J. Oldham. 2016. Prototype e-cigarette and the capillary aerosol generator (CAG) comparison and qualification for use in subchronic inhalation exposure testing. *Aerosol Sci. Technol.* 50 (12):1284–93. doi:10.1080/02786826.2016.1219017.

Williams, M., and P. Talbot. 2019. Design features in multiple generations of electronic cigarette atomizers. *IJERPH.* 16 (16):2904. doi:10.3390/ijerph16162904.

Yingst, J. M., C. Lester, S. Veldheer, S. I. Allen, P. Du, and J. Foulds. 2019. E-cigarette users commonly stealth vape in places where e-cigarette use is prohibited. *Tob. Control.* 28 (5):493–7. doi:10.1136/tobaccocontrol-2018-054432.

Zhao, T., S. Shu, Q. Guo, and Y. Zhu. 2016. Effects of design parameters and puff topography on heating coil temperature and mainstream aerosols in electronic cigarettes. *Atmos. Environ.* 134:61–9. doi:10.1016/j.atmosenv.2016.03.027.

Zhao, Z., M. Zhang, J. Wu, X. Xu, P. Yin, Z. Huang, X. Zhang, Y. Zhou, X. Zhang, C. Li, et al. 2020. E-cigarette use among adults in China: Findings from repeated cross-sectional surveys in 2015–16 and 2018–19. *Lancet. Public Health.* 5 (12):e639–e649. doi:10.1016/S2468-2667(20)30145-6.

Zhou, Y., H. Irshad, W. W. Dye, G. Wu, C. S. Tellez, and S. A. Belinsky. 2021. Voltage and e-liquid composition affect nicotine deposition within the oral cavity and carbonyl formation. *Tob. Control.* 30 (5):485–91. doi:10.1136/tobaccocontrol-2020-055619.